ACCURATE ANALYSIS METHOD OF BACKGROUND IONOSPHERE EFFECTS ON GEOSYNCHRONOUS SAR FOCUSING

Ye Tian, Cheng Hu, Kai Zhang, Teng Long and Tao Zeng

School of Information and Electronics, Beijing Institute of Technology
Beijing, 100081, P.R. China

ABSTRACT

The background ionosphere time variance within the extremely long integration time of Geosynchronous Synthetic Aperture Radar (GEO SAR) needs to be considered for GEO SAR focusing. Meanwhile, because of the curved trajectory and the very complex geometry relationship between satellite motion and earth rotation, the traditional analysis method of background ionosphere on LEO SAR imaging will no longer suitable in GEO SAR. In this paper, a GEO SAR signal model is proposed to describe the effects of total electron content (TEC) variance within the long integration time. Then, a GEO SAR signal two-dimensional spectrum under the effects of background ionosphere is derived for the first time. The GEO SAR defocusing phase errors are derived analytically. At last, the US Total Electron Content (US-TEC) data are used and the focusing results are presented, verifying the analysis.

Index Terms— GEO SAR，Background Ionosphere，Focusing

1. INTRODUCTION

Geosynchronous Synthetic Aperture Radar (GEO SAR), running in the height of 36000 km geosynchronous earth orbit, compared with traditional Low Earth Orbit (LEO) SAR (orbit height under 1000 km), GEO SAR has advantages of shorter repeat period, wider swath and so on. A single GEO SAR can cover one third of the global surface, resulting in the short revisiting time, even less than 24 hours. Most of the literature about GEO SAR is focused on the imaging technology, system parameters design, atmosphere effects, and applications. K. Tomiyasu put forward the concept of GEO SAR firstly and analyzed some primary parameters [1]. Hobbs et al. studied the GEO SAR configuration and designed the system parameters [2]. Ruiz Rodon, J et al researched the effects of atmosphere on GEO SAR system [3]. As for the signal characteristics and imaging algorithms, the related literature is mainly concentrated on the modification of conventional SAR imaging algorithms in GEO SAR [4], such as modified Secondary Range Compression (SRC) algorithm, modified Chirp Scaling (CS) algorithm and so on.

So far, few literatures are related to the effects of ionosphere on GEO SAR imaging [5]. In this paper, a GEO SAR signal model is proposed to describe the effects of ionosphere. The mathematical expressions of the signal two-dimensional spectrum of GEO SAR induced by background ionosphere are derived. Then, the effects of background ionosphere on range and azimuth focusing are analyzed. Finally, the USTEC data are acquired and modified for imaging. The focusing results verify the theoretical analysis.

2. GEO SAR SIGNAL MODEL INFLUENCED BY BACKGROUND IONOSPHERE

2.1. Accurate Range Model of GEO SAR

Because of the characteristics of long integration time and high orbit height, and the very complex geometry relationship between satellite motion and earth rotation in GEO SAR, the conventional range model will no longer suitable for GEO SAR, it is necessary to build a new accurate GEO SAR range model.

GEO SAR runs in the height of 36000 km geosynchronous earth ellipse orbit in 3-dimensional (3D) space. The geometry model of GEO SAR is shown as Fig. 1.

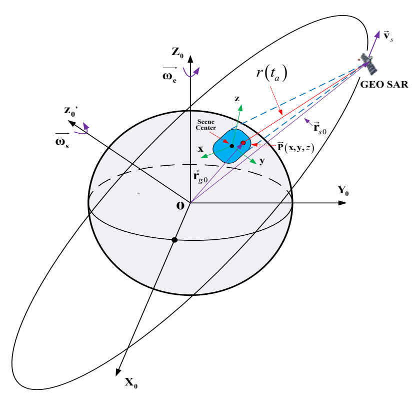

Fig. 1 Geometry and signal model of GEO SAR

In Fig. 1, O-XYZ is the scene coordinate system, $\overline{P}(x,y,z)$ is the location vector of target P. $r(t_a)$ is the true instant slant range at t_a from satellite to target point $\overline{P}$, $\overline{V}_s$ is the GEO SAR satellite velocity. $\vec{\mathbf{r}}_{s0}$ and $\vec{\mathbf{r}}_{g0}$ are the satellite position vector and target position vector at aperture center moment in O-XYZ respectively.

According to the analysis of literature [4], the accurate range model of GEO SAR can be expressed as

$$\begin{aligned} r(t_a) &= \left\|\vec{\mathbf{r}}_s(t_a) - \vec{\mathbf{r}}_g(t_a)\right\| \\ &= r_0 + q_1 \cdot (t_a) + q_2 \cdot (t_a)^2 + q_3 \cdot (t_a)^3 + \cdots \end{aligned} \tag{1}$$

where, $\vec{\mathbf{r}}_g(t_a)$ is the target position vector at t_a, $\vec{\mathbf{r}}_s(t_a)$ is the satellite position vector at t_a. r_0 is the distance from the satellite to reference point at aperture center moment. $q_1 \sim q_3$ are the first to third order derivatives of r_n and their specific expressions are

$$r_0 = \left\|\vec{\mathbf{r}}_{s0} - \vec{\mathbf{r}}_{g0}\right\| \tag{2}$$

$$q_1 = \left(\vec{\mathbf{v}}_{s0} - \vec{\mathbf{v}}_{g0}\right) \cdot \left(\vec{\mathbf{r}}_{s0} - \vec{\mathbf{r}}_{g0}\right)^{\mathrm{T}} \Big/ \left\|\vec{\mathbf{r}}_{s0} - \vec{\mathbf{r}}_{g0}\right\| \tag{3}$$

$$\begin{aligned} q_2 = &\frac{\left(\vec{\mathbf{a}}_{s0} - \vec{\mathbf{a}}_{g0}\right) \cdot \left(\vec{\mathbf{r}}_{s0} - \vec{\mathbf{r}}_{g0}\right)^{\mathrm{T}} + \left\|\vec{\mathbf{v}}_{s0} - \vec{\mathbf{v}}_{g0}\right\|^2}{2 \cdot \left\|\vec{\mathbf{r}}_{s0} - \vec{\mathbf{r}}_{g0}\right\|} \\ &- \frac{\left[\left(\vec{\mathbf{v}}_{s0} - \vec{\mathbf{v}}_{g0}\right) \cdot \left(\vec{\mathbf{r}}_{s0} - \vec{\mathbf{r}}_{g0}\right)^{\mathrm{T}}\right]^2}{2 \cdot \left\|\vec{\mathbf{r}}_{s0} - \vec{\mathbf{r}}_{g0}\right\|^3} \end{aligned} \tag{4}$$

$$\begin{aligned} q_3 = &\frac{\left(\vec{\mathbf{b}}_{s0} - \vec{\mathbf{b}}_{g0}\right) \cdot \left(\vec{\mathbf{r}}_{s0} - \vec{\mathbf{r}}_{g0}\right)^{\mathrm{T}} + 3 \cdot \left(\vec{\mathbf{a}}_{s0} - \vec{\mathbf{a}}_{g0}\right) \cdot \left(\vec{\mathbf{v}}_{s0} - \vec{\mathbf{v}}_{g0}\right)^{\mathrm{T}}}{6 \cdot \left\|\vec{\mathbf{r}}_{s0} - \vec{\mathbf{r}}_{g0}\right\|} \\ &- \frac{\left(\vec{\mathbf{v}}_{s0} - \vec{\mathbf{v}}_{g0}\right) \cdot \left(\vec{\mathbf{r}}_{s0} - \vec{\mathbf{r}}_{g0}\right)^{\mathrm{T}} \cdot \left(\vec{\mathbf{a}}_{s0} - \vec{\mathbf{a}}_{g0}\right) \cdot \left(\vec{\mathbf{r}}_{s0} - \vec{\mathbf{r}}_{g0}\right)^{\mathrm{T}}}{2 \cdot \left\|\vec{\mathbf{r}}_{s0} - \vec{\mathbf{r}}_{g0}\right\|^3} \\ &- \frac{\left(\vec{\mathbf{v}}_{s0} - \vec{\mathbf{v}}_{g0}\right) \cdot \left(\vec{\mathbf{r}}_{s0} - \vec{\mathbf{r}}_{g0}\right)^{\mathrm{T}} \cdot \left\|\vec{\mathbf{v}}_{s0} - \vec{\mathbf{v}}_{g0}\right\|^2}{2 \cdot \left\|\vec{\mathbf{r}}_{s0} - \vec{\mathbf{r}}_{g0}\right\|^3} \\ &+ \frac{\left[\left(\vec{\mathbf{v}}_{s0} - \vec{\mathbf{v}}_{g0}\right) \cdot \left(\vec{\mathbf{r}}_{s0} - \vec{\mathbf{r}}_{g0}\right)^{\mathrm{T}}\right]^3}{2 \cdot \left\|\vec{\mathbf{r}}_{s0} - \vec{\mathbf{r}}_{g0}\right\|^5} \end{aligned} \tag{5}$$

where, $\vec{\mathbf{v}}_{s0}$ is the satellite velocity vector at aperture center moment. $\mathbf{R_0}$ is the distance from the satellite to reference point at aperture center moment. $\vec{\mathbf{a}}_{s0}$, $\vec{\mathbf{b}}_{s0}$ and $\vec{\mathbf{d}}_{s0}$ are the acceleration velocity vector, the derivate of $\vec{\mathbf{a}}_{s0}$ and the derivate of $\vec{\mathbf{b}}_{s0}$ at aperture center moment respectively.

The conventional range model will be substituted by the range model of equations (1)~(5) in the following parts.

2.2. Background Ionosphere Effects on GEO SAR Signal

When SAR signals pass through the background ionosphere, the phase error will be generated under the influence of background ionosphere [6]

$$\Delta\phi = -\frac{4\pi(\Delta t \cdot c)}{\lambda} \approx -\frac{2\pi \cdot 80.6 \cdot TEC}{c \cdot f} \tag{6}$$

where, TEC is the total electron content, f is signal frequency, c is light speed. As GEO SAR transmit chirp signal, equation (6) can be expressed as

$$\Delta\phi = -\frac{2\pi \cdot 80.6 \cdot TEC}{c \cdot (f_0 + f_r)} \tag{7}$$

where, f_0 is center frequency, f_r is range frequency. As the integration time of GEO SAR increases significantly and reaches hundreds of seconds' level compared with LEO SAR [4], TEC within integration time will no longer be a constant value and varies with integration time.

Therefore, The TEC variance in long integration time can be expressed as function of slow time t_a

$$TEC(t_a) = TEC_0 + \Delta TEC(t_a) \tag{8}$$

where, TEC_0 is the constant part and $TEC(t_a)$ varies along with integration time which can be expanded as the Taylor series

$$\Delta TEC = k_1 \cdot t_a + k_2 \cdot t_a{}^2 + k_3 \cdot t_a{}^3 + \cdots \tag{9}$$

where, k_i is the derivative of each order of TEC.

2.3. GEO SAR Signal Model and Its Two-dimensional Spectrum Under the Effects of Background Ionosphere

Based on Fig. 1, the expression of GEO SAR echo is

$$s(t_a,t) = A_r(t) \cdot A_a(t_a) \cdot \exp\left[j\pi k_r \left(t - \frac{2r(t_a)}{c}\right)^2\right] \cdot \exp\left[-j4\pi \frac{r(t_a)}{\lambda}\right] \tag{10}$$

where, $A_r(\cdot)$ and $A_a(\cdot)$ are signal range and azimuth envelope respectively, k_r is chirp rate, λ is signal wavelength, t is fast time, ta is slow time. Operate range FFT to equation (10) and consider the additional phase error induced by background ionosphere, the expression of influenced echo can be expressed as

$$\begin{aligned} S(f_r,t_a) = &A_r(f_r) \cdot A_a(t_a) \cdot \exp\left[-j\frac{4\pi(f_r + f_0) \cdot r(t_a)}{c}\right] \\ &\cdot \exp\left(-j\frac{\pi f_r^2}{k_r}\right) \cdot \exp(j \cdot \Delta\phi) \end{aligned} \tag{11}$$

where, the specific expression of $\Delta\phi$ is shown as (7).

Operate Fourier transform to (11) by using series reversion method. The GEO SAR signal two-dimensional spectrum influenced by background ionosphere can be drawn as

$$S(f_a,f_r)=$$
$$\sigma A_a(f_a)A_r(f_r)\cdot\exp\left(-j\cdot\pi\frac{f_r^2}{\beta}\right)$$
$$\times\exp\left(-j\cdot 2\pi\cdot\frac{2(f_r+f_0)}{c}\cdot\left(r_0+\frac{40.3\cdot TEC_0}{(f_0+f_r)^2}\right)\right)$$
$$\times\exp\left(j\cdot 2\pi\cdot\frac{1}{4\cdot\left(q_2+\frac{40.3\cdot k_2}{f_0^2}\right)}\cdot\frac{c}{2(f_r+f_0)}\cdot\left(f_a+\frac{2\cdot(f_r+f_c)}{c}\cdot\left(q_1+\frac{40.3\cdot k_1}{f_0^2}\right)\right)^2\right)$$
$$\times\exp\left(j\cdot 2\pi\cdot\frac{q_3+\frac{40.3\cdot k_3}{f_0^2}}{8\cdot\left(q_2+\frac{40.3\cdot k_2}{f_0^2}\right)^3}\cdot\left(\frac{c}{2(f_r+f_0)}\right)^2\cdot\left(f_a+\frac{2\cdot(f_r+f_c)}{c}\cdot\left(q_1+\frac{40.3\cdot k_1}{f_0^2}\right)\right)^3\right) \quad (12)$$

Based on (12), the specific effects of background ionosphere on GEO SAR focusing will be analyzed in the following part.

3. IMPACTS ANALYSIS OF BACKGROUND IONOSPHERE ON GEO SAR FOCUSING

In order to analyze the impact of background ionosphere on GEO SAR focusing, Taylor expansion will be used in equation (12) with respect to the range frequency $f_r=0$. Then, the range and azimuth phase errors induced by background ionosphere can be obtained.

3.1. Effects on GEO SAR Focusing in Range Direction

The quadratic phase error (QPE) in range direction will deteriorate the range focusing performance by broadening the main-lobe and raising the side-lobe. The expression of range QPE is

$$\phi_{range2}=\frac{2\pi}{cf_0}\cdot\left(-\frac{80.6\cdot TEC_0}{f_0^2}+\left(\frac{\left(q_1+\frac{40.3k_1}{f_0^2}\right)^3\left(q_3+\frac{40.3k_3}{f_0^2}\right)}{16\cdot\left(q_2+\frac{40.3k_2}{f_0^2}\right)^3}-\frac{q_1^3\cdot q_3}{16\cdot q_2^3}\right)\right)\cdot B^2 \quad (13)$$

Where, B is signal bandwidth

The cubic phase error (CPE) in range direction will influence focusing by introducing asymmetry side-lobes. The expression of range CPE is

$$\phi_{range3}=\frac{2\pi}{cf_0^2}\cdot\left(\frac{80.6\cdot TEC_0}{f_0^2}+\left(\frac{\left(q_1+\frac{40.3k_1}{f_0^2}\right)^3\left(q_3+\frac{40.3k_3}{f_0^2}\right)}{16\cdot\left(q_2+\frac{40.3k_2}{f_0^2}\right)^3}-\frac{q_1^3\cdot q_3}{16\cdot q_2^3}\right)\right)\cdot B^3 \quad (14)$$

According to (13) and (14), the range QPE and CPE are related to the constant and varying part of TEC. Their maximum values are proportional to signal bandwidth, constant and varying part of TEC, and inversely proportional to signal frequency.

3.2. Effects on GEO SAR Focusing in Azimuth Direction

Within the entire azimuth frequency band, the signal part within the range of the azimuth bandwidth is only the one that authentically affects focusing. Therefore, substituting the azimuth frequency f_a with the azimuth bandwidth B_a, the azimuth signal bandwidth $B_a=f_{dr}\cdot T_a$, T_a is integration time, f_{dr} is azimuth FM rate. The azimuth QPE caused by the background ionosphere is

$$\phi_{azimuth2}=$$
$$\frac{\pi c}{f_0}\cdot\left(\frac{1}{\left(q_2+\frac{40.3k_2}{f_0^2}\right)}\cdot\left(\frac{1}{4}+\frac{3\left(q_1+\frac{40.3k_1}{f_0^2}\right)\left(q_3+\frac{40.3k_3}{f_0^2}\right)}{8\left(q_2+\frac{40.3k_2}{f_0^2}\right)^2}\right)-\frac{1}{q_2}\cdot\left(\frac{1}{4}+\frac{3\cdot q_1q_3}{8\cdot q_2^2}\right)\right)\cdot(f_{dr}\cdot T_a)^2 \quad (15)$$

The azimuth CPE caused by the background ionosphere is

$$\phi_{azimuth3}=\frac{\pi c^2}{16f_0^2}\cdot\left(\frac{\left(q_3+\frac{40.3k_3}{f_0^2}\right)}{\left(q_2+\frac{40.3k_2}{f_0^2}\right)^3}-\frac{q_3}{q_2^3}\right)\cdot(f_{dr}\cdot T_a)^3 \quad (16)$$

The azimuth QPE and CPE will result in azimuth defocusing, and the defocusing level will deteriorate as the increase of integration time.

4. SIMULATION AND PERFORMANCE ANALYSIS

In this part, the US Total Electron Content (US-TEC) [7] is used to verify the theoretical analysis. The USTEC data are acquired in October 7th 2013, 18:00 p.m. at 39.36^{0}N, 98.85^{0}W. The GEO SAR parameters are listed in Table. 1.

As the data are updated every 15 minutes, the Lagrange's interpolation is used to obtain desired TEC. The modified TEC data are updated every second as shown in Fig. 2.

According to equations (8) and (9) and the USTEC data in Fig. 2, the first order derivative of TEC is 0.0068 TECU/S, the second order derivative of TEC is 7.32×10^{-6} TECU/S^2, and the third order derivative of TEC is 1.65×10^{-9} TECU/S^3.

Table. 1 GEO SAR system parameters

Item	Value	Item	Value
Orbit Height/km	35578.8	Semi-major Axies/km	42164.2
Inclination/^{0}	53	Eccentricity	0.07
Argument of Perigee/^{0}	270	Right Ascension of Ascending Node/^{0}	265
Antenna Size/m	30	Wavelength/m	0.24
Bandwidth/MHz	18	Sampling Rate/MHz	20

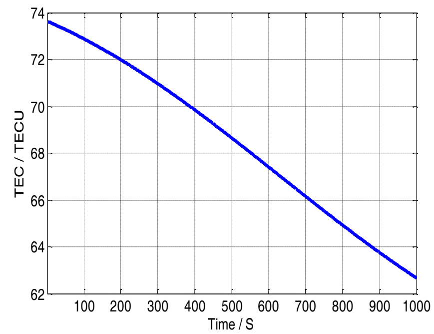

Fig. 2 TEC variance within 1000 s (acquired from USTEC)

The focusing results are shown in Fig. 3. As the defocusing level will deteriorate as the increase of integration time, the integration time is set to 100 s, 300 s and 500 s.

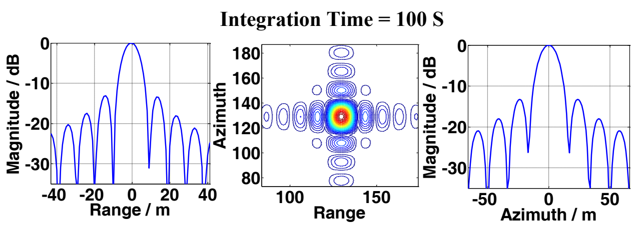

a (Left: range profile; Right: azimuth profile)

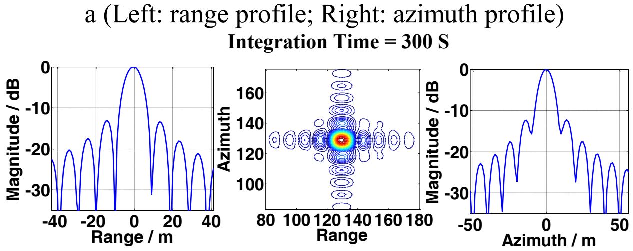

b (Left: range profile; Right: azimuth profile)

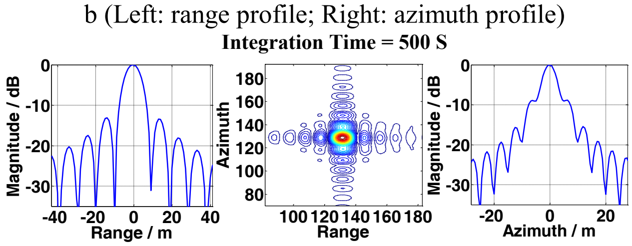

c (Left: range profile; Right: azimuth profile)

Fig. 3 GEO SAR focusing resluts within various integration time using the USTEC data and GEO SAR parameters

Usually in SAR focusing, if the QPE less than 0.78 radians or the CPE less than 0.39 radians, it will not cause defocusing. So, based on (13)(14) and the US-TEC data, the range QPE and CPE are 0.29 radians and 0.041 radians respectively, thus the range profiles are perfect. Meanwhile, based on (15)(16) and the US-TEC data, the maximum integration time under un-defocusing condition is 171.35 s. In Fig. 3-a, the integration time is less than 171.35 s, thus the azimuth profile is perfect. However, in Fig. 3-b and c, the integration times are greater than 171.35 s, thus the azimuth profiles are defocusing, and the greater the integration time is, the worse the defocusing azimuth profile is.

5. CONCLUSIONS

This paper analyzes the impact of background ionosphere on GEO SAR focusing. Based on accurate GEO SAR range model and the phase error induced by TEC within integration time, the signal two-dimensional spectrum influenced by background ionosphere is obtained. The GEO SAR range and azimuth phase errors are derived analytically and their specific effects are analyzed. The range and azimuth defocusing are worse as the increase of signal bandwidth and integration time respectively. The US-TEC data are used to analyze the effects of background ionosphere on GEO SAR focusing and the theoretical analysis is verified. In future, the compensation of background ionosphere will be the main research work, such as phase gradient autofocus (PGA) algorithm and so on.

6. ACKNOWLEDGEMENTS

This work was supported by the National Natural Science Foundation of China (NSFC) under Grant Nos. 61032009, 61225005 and 61120106004, and 111 project of China under grant B14010.

7. REFERENCES

[1] K. Tomiyasu, “Synthetic aperture radar in geosynchronous orbit”, in *Proc. IEEE Antennas and Propagation Symp.*, pp. 42-45, 1978.

[2] D. Bruno and S.E. Hobbs, “Radar imaging from geosynchronous orbit: temporal decorrelation aspects”, *IEEE Trans. Geosci. Remote Sens.*, vol.48, no.7, pp.2924-2929, 2010

[3] J. R. Rodon, A. Broquetas and A.M. Guarnieri, “Geosynchronous SAR Focusing With Atmospheric Phase Screen Retrieval and Compensation”, *IEEE Trans. Geosci. Remote Sens.*, 2013, 51, (8), pp.4397-4404.

[4] C. Hu, T. Long, Z.P. Liu, T. Zeng and Y. Tian, “An Improved Frequency Domain Focusing Method in Geosynchronous SAR,” *IEEE Trans. Geosci. Remote Sens.*, vol.52, no.9, pp.5514-5528, Sep. 2014.

[5] F.J. Meyer, “Performance Requirements for Ionospheric Correction of Low-Frequency SAR Data”, *IEEE Trans. Geosci. Remote Sens.*, vol.49, no.10, pp.3694-3702, Oct 2011.

[6] Z.W.Xu, J.Wu and Z.S.Wu, “A survey of ionosphere effects on space-based radar”, *Waves Random Media*, Vol.14, No.2, pp.189-273, Apr.2004.

[7] NOAA/Space Weather Prediction Center; Vertical Total Electron Content; http://www.swpc.noaa.gov/ustec/; Oct 2013.